

Strongly correlated excitation of a quasi-1D Rydberg gas

N Malossi^{a,b,1}, M M Valado^{a,b}, S Scotto^{a,2}, O Morsch^{a,b}, E Arimondo^{a,b,c} and D Ciampini^{a,b,c}

^a Dipartimento di Fisica ‘E. Fermi’, Università di Pisa, Largo Pontecorvo 3, 56127 Pisa, IT

^b INO-CNR, Via G. Moruzzi 1, 56124 Pisa, IT

^c CNISM UdR Pisa, Dipartimento di Fisica ‘E. Fermi’, Università di Pisa, Largo Pontecorvo 3, 56127 Pisa, IT

E-mail: ciampini@df.unipi.it

Abstract. Rydberg excitation dynamics of a 87-Rb cold atom cloud is investigated in an effective one-dimensional geometry. We measure the excitation dynamics and the full counting statistics for resonant and off-resonant excitation to the $70S$ state. While for a resonant laser excitation the counting distributions have a strong sub-Poissonian character, we find strongly bimodal counting distributions in the off-resonant regime. The n -th central moments, up to $n = 4$, of the counting distributions are derived from the measured counting distributions.

1. Introduction

Atoms in high-lying Rydberg states strongly interact with each other via the dipole-dipole or van-der-Waals potential [1, 2, 3]. The interaction-induced level shifts can suppress resonant optical excitation of more than one Rydberg atom within a certain blockade volume containing tens or hundreds of atoms [3, 4]. This long-range interaction is at the heart of many quantum information processing schemes [5, 6] including quantum gates between individual atoms [7, 8, 9, 10]. A system of strongly interacting Rydberg atoms holds also promise for studies of dynamics and disorder in many-body systems with tunable interactions. Dynamical crystallisation with long range order over the full sample can be produced by the application of properly shaped laser pulses [11, 12]. The short-range organisation of Rydberg excitation was recently observed for Rydberg atoms created in an optical lattice [13].

For resonant laser excitation an important consequence of the dipole blockade is the suppression of fluctuations in the number of Rydberg excitations [14, 15, 16, 17], leading to highly sub-Poissonian excitation statistics with a negative large Mandel Q -parameter [18]. Such fluctuation suppression evidences the creation of quantum correlations in the whole sample.

The present work reports experimental observations for the off-resonant excitation scheme, with the excitation laser having a finite detuning from the Rydberg state. In such an off-resonant excitation scheme, a pair of atoms undergoes a pair excitation if the atomic interaction matches

¹ Present address: Scuola di Scienze e Tecnologie, Sezione di Fisica, Università di Camerino, I-62032 (MC), IT.

² Present address: Laboratoire National des Champs Magnétiques Intenses (UPR 3228, CNRS-UPS-UJF-INSA), 31400 Toulouse, FR.



the laser energy defect/excess. After such event, neighbouring ground-state atoms at the resonant distance have an enhanced excitation probability, owing to the interaction induced energy shifts. As a consequence an already excited Rydberg atom pair can shift other atoms into resonance, in a domino effect, leading to an increasing overall Rydberg excitation probability. We demonstrate that the strong atomic correlations result in a super-Poissonian excitation statistics with positive Mandel Q -parameter. The off-resonant excitation of Rydberg pairs was examined by previous authors [19, 20] without a study of the excitation statistics. A super-Poissonian statistics was observed for a quantum dot optically coupled to a detuned cavity, where the cooling of initial photons is inhibited, but once an initial photon is coupled the coupling of subsequent photons is increased via multiphoton processes [21]. In the investigation of single-electron tunneling in semiconductor quantum dots, the ability to detect individual charges in real-time makes it possible to count electrons, measure their counting statistics and investigate correlations between charge carriers [22].

Both resonant and off-resonant Rydberg excitation produce strong spatial and temporal correlations in the sample, created by the long-range interactions [16, 17, 23, 24]. In this work we study the interaction dynamics of Rydberg atoms in an effective 1D geometry in which excitations can occur only along one spatial direction. The dynamics in the off-resonant excitation regime is governed by a complex interplay between off-resonant single-atom and pair excitations mediated by the Rydberg-Rydberg interaction. Our measured Rydberg counting distribution shows a bimodal structure, with a peak at zero excitations corresponding to the probability that no pairs of atoms have been excited and a second peak at a large number of excitations, as reproduced by our theoretical analysis based on a Dicke-type model, described in [24].

2. Rydberg blockade

The $5S$ atoms are excited to the $70S$ Rydberg state using a two-photon excitation process with detuning via the intermediate $6P$ level (see [25, 16, 26] for details). In the Rydberg excitation scheme the excitation lasers are detuned by 2 GHz from the $6P$ state, which can therefore be adiabatically eliminated and the laser interaction will be described by a two-level effective system with Rabi frequency Ω and laser detuning Δ . Since rubidium atoms in the $70S$ state have repulsive interactions described by the van-der-Waals coefficient $C_6 > 0$, a positive interaction energy has to be added to the excitation energy. The ensemble of N_{db}^{at} atoms within the blockade radius volume, carrying only one excitation that can be located at any of the atoms, is excited collectively to a Wigner state, evolving with a collective Rabi frequency $\Omega^{coll} = \sqrt{N_{db}^{at}}\Omega$ [3, 27]

For an off-resonant excitation using a laser detuned by Δ from the singly-Rydberg excited state, a pair of Rydberg atoms at distance R can be excited, if the pair van-der-Waals interaction energy matches twice the energy mismatch $\hbar\Delta$ of the laser excitation, i.e., $C_6/R^6 = 2\hbar\Delta$. The timescale for the off-resonant excitation of a single atom pair is determined by the Rabi frequency $\Omega_{off} = \Omega^2/(2\Delta)$ of this two-atom two-photon process.

3. Experimental realization

In our experiment we create small clouds of ultracold 87-Rb atoms in a magneto-optical trap (MOT). The cold cloud has approximately a Gaussian density profile with typical widths $\sigma = 40 \mu\text{m}$ and containing $N^{at} = 4 \times 10^4$ atoms. The resulting peak density, $n = 5 \times 10^{10} \text{ cm}^{-3}$, corresponds to a mean inter-particle spacing of around $2.6 \mu\text{m}$. The first step laser at 420 nm is sent through a single mode optical fiber and focused to a $w = 6 \mu\text{m}$ Gaussian waist, which is smaller than the dipole blockade radius for the $70S$ state. As a consequence, the probability to excite more than one atom in the radial direction is suppressed by the exponentially decreasing two-photon Rabi frequency as a function of the radial coordinate r ($\Omega(r) \propto e^{-2r^2/w^2}$) and hence the Rydberg excitations are created in an effective 1D geometry. The second step laser at

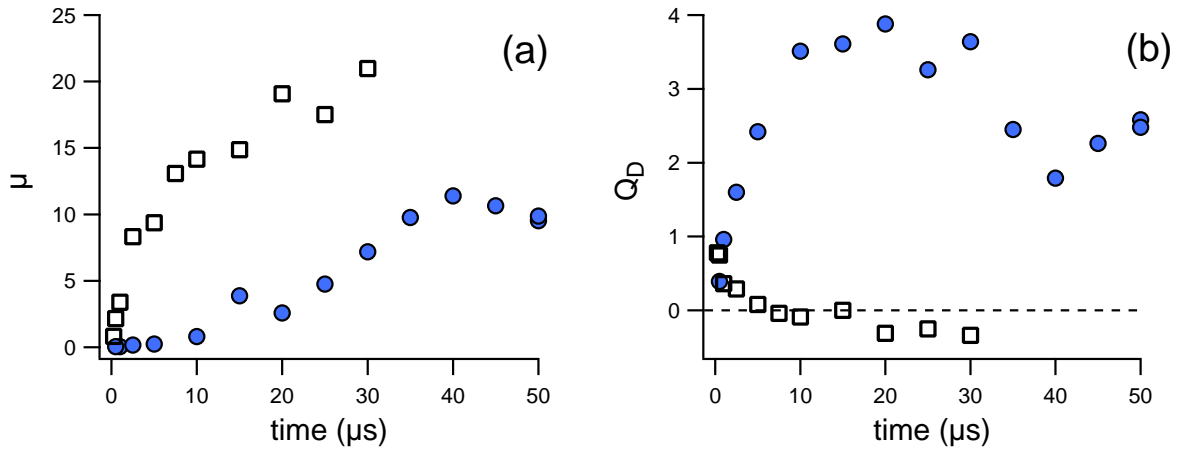


Figure 1. Experimental results for 70S excitation dynamics and statistics of the detected ions for resonant ($\Delta = 0$) and off-resonant excitation ($\Delta/2\pi = 7.7$ MHz). Detected ion mean number, in (a), and detected Mandel Q -factor of the detected ions, in (b), vs excitation time. Black open squares for on resonance and blue full circles for off-resonance.

1013 nm has a Gaussian waist of $80 \mu\text{m}$, larger than the MOT size. For the atoms in the highest laser intensity region $\Omega/2\pi$ is 900 kHz. For our number $N_{db}^{at} \approx 20$ of atoms inside the blockade volume, the resonant collective Rabi frequency is $\Omega^{coll} = \sqrt{N_{db}^{at}}\Omega \approx 2\pi \times 4$ MHz.

For the $\Delta/2\pi = 7.7$ MHz detuning of the present investigation, the resonance condition for pair excitation corresponds to an interatomic separation of $R = 6.5 \mu\text{m}$, comparable with w , the Gaussian beam waist of the blue excitation laser. The off-resonant excitation timescale is given by $\Omega_{off} \approx 2\pi \times 50$ kHz in the highest laser intensity region. Ω_{off} is proportional to the intensity of the blue laser and quickly decreases in the radial direction, as $\Omega_{off}(r) \propto e^{-4r^2/w^2}$. Therefore, for both the resonant and off-resonant excitations our system can be considered as an effective quasi-1D system.

After the excitation pulse (of duration between 0.2 and $50 \mu\text{s}$) an electric field is applied for $2 \mu\text{s}$ in order to field ionize the Rydberg atoms and to accelerate the resulting ions towards a channeltron. The overall detection efficiency is $\eta \approx 40\%$ [25]. During the entire excitation and detection sequence the MOT beams are switched off. The excitation-detection cycle is repeated 500 times, in order to measure the counting distribution of the detected ions. The experiments described in this paper are in the non-dissipative regime, since the longest excitation time used here ($50 \mu\text{s}$) is shorter than the Rydberg state lifetime ($\sim 200 \mu\text{s}$ for the 70S state). On the other hand, since the excitation times are typically longer than the coherence time of the laser (limited by the finite linewidth of the excitation laser of approximately 0.5 MHz), most of the system dynamics takes place in an incoherent regime.

4. Results

From the counting distributions of the detected ions we derived the probability $P(N_{ion}, t)$ for the detection of N_{ion} after an interaction time t for resonant and off-resonant excitation. From that probability we calculated the n -th order central moments $\mu_n = \langle (N_{ion} - \mu)^n \rangle$ up to $n = 4$ as well as their associated normalized quantities Mandel Q -factor $Q_D = \mu_2/\mu - 1$, Binder cumulant $B_D = 1 - \mu_4/(3\mu_2^2)$ and bimodality coefficient $b_D = (\gamma^2 + 1)/(\mu_4/\mu_2^2)$ as a function of the mean number μ . For the purposes of this paper, we focus on the 2nd and 4th order moments. All the

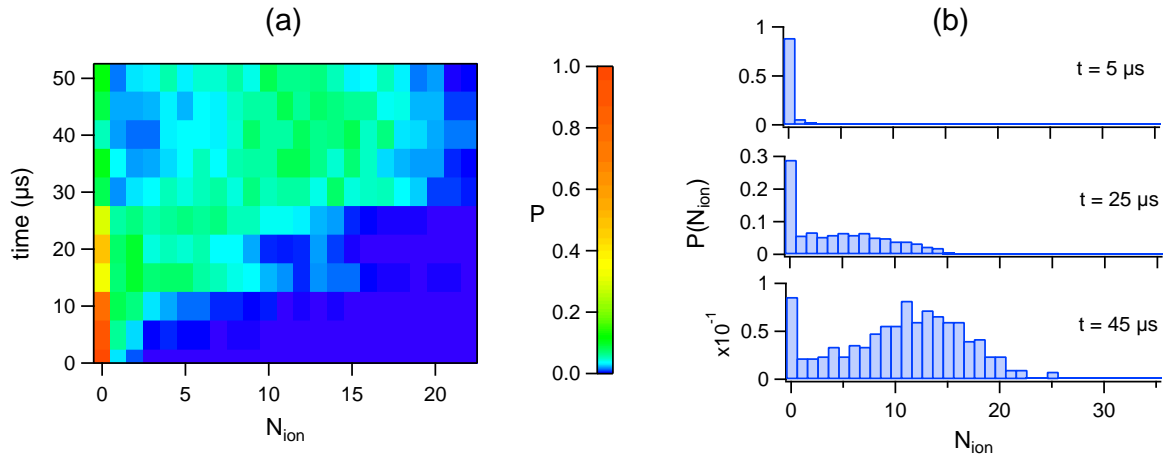


Figure 2. Histograms of $P(N_{ion}, t)$ vs interaction time t in the $\Delta/2\pi = 7.7$ MHz off-resonant regime. In (a) global evolution of $P(N_{ion}, t)$ highlighted by a false color representation. In (b) histograms for excitation times $t = 5, 25$ and $45 \mu s$.

above quantities are calculated from the *observed* counting distribution, i.e., the distribution of the detected ions, and the finite detection efficiency has to be taken into account for the comparison with a theoretical model (see [24] for details). For the Mandel Q -factor the simple relation $Q_D = \eta Q$ between the detected quantity and the actual one holds.

The mean number of detected ions and the detected Mandel Q -parameter are shown in Fig.1. For a $\Delta = 0$ resonant excitation, a rapid increase in the average detected ion number is concomitant with a decrease in Q_D . After few microseconds the growth in the detected ion number slows down while Q_D fluctuates around -0.3 , illustrating the sub-Poissonian character of the distribution on resonance. For the $\Delta/2\pi = 7.7$ MHz off-resonant excitation, the mean number of detected ions grows much more slowly than in the resonant case, since $\Omega_{off} \ll \Omega$. The maximum value is approximately half the number of detected ions in the resonant saturated regime. In that regime the Mandel Q -parameter is large and positive, showing the super-Poissonian nature of the counting distribution.

In Fig. 2 histograms of $P(N_{ion}, t)$ in the off-resonant excitation regime are presented. The false-color representation of Fig. 2(a) provides a global view, while histograms of $P(N_{ion}, t)$ vs N_{ion} for different excitation t times are shown in Fig. 2(b). The bimodality of the ion distribution is highlighted in Fig. 2(a) and appears clearly in the plot of Fig. 2(b) at $t = 45 \mu s$.

In Fig. 3 several statistical quantities derived from the off-resonant and resonant counting distributions are shown as a function of the mean number of detected ions. These plots allow a direct comparison between the on- and off-resonant excitation regimes for equal excitation numbers, independently of their very different timescales. In Fig. 3(a) and (b) the variance and the Mandel Q -parameter are shown. For resonant excitation, the variance grows in the full explored range of parameters and the Mandel Q -factor becomes negative when the saturation is approached. For off-resonant excitation, the variance reaches its maximum for the largest number of detected ions reported in Fig. 1(a). The Mandel parameter Q_D reaches its maximum at smaller values of detected ions because it is obtained from the variance applying a normalization by the mean number. Figure 3(c) shows the bimodality parameter as a function of the mean number of detected ions. In the explored range, it is always larger for off-resonant excitation, emphasizing the qualitatively different nature of the on- and off-resonant counting distributions. Figure 3(d) reports the values of the Binder cumulant for resonant and off-resonant

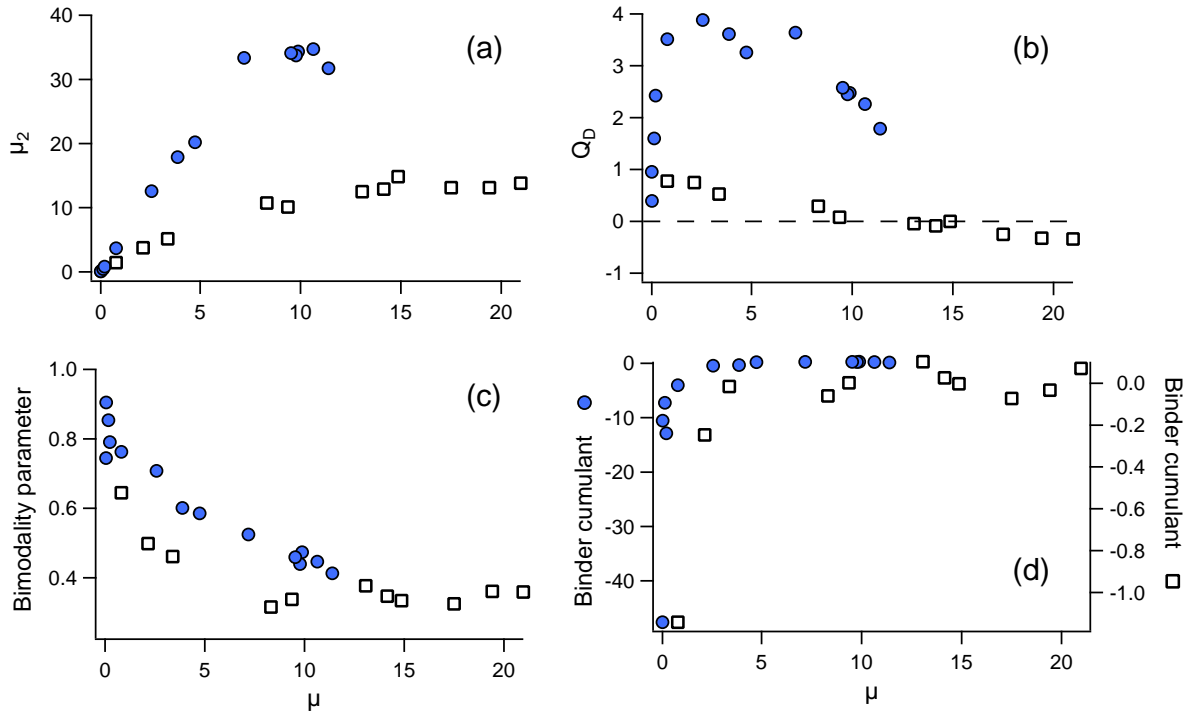


Figure 3. Statistical quantities calculated from the off-resonant (blue full circles) and resonant (black open squares) counting distributions are shown as a function of the mean number of detected ions. In (a) second-order moment μ_2 , in (b) Mandel Q -factor, in (c) bimodality parameter, in (d) the Binder cumulant. The off-resonant excitation detuning is $\Delta/2\pi = 7.7$ MHz.

excitation. As originally pointed out by Binder [28], this quantity allows one to extract the critical parameters and the critical exponents for a system experiencing a phase transition, for instance the Ising quantum phase transition predicted for Rydberg experimental configurations in [29, 30, 31].

5. Conclusions

We have studied strongly correlated Rydberg excitations in an effective 1D geometry. Our system is quasi-1D for both resonant excitation and also the off-resonant excitation at the explored detuning from the $70S$ state. The explored excitation times are longer than the coherence time, limited by the finite linewidth of the excitation lasers, but shorter than the Rydberg lifetime. Therefore the presented experimental observations take place in an incoherent regime, but not in the dissipative regime explored in [24].

We have measured the full counting statistics of the Rydberg excitations and derived from the statistical distributions the central moments up to $n = 4$. The counting distribution at resonance is characterized by a strong sub-Poissonian character, while in the off-resonant regime the histograms of the counting distribution are clearly bimodal. The statistical moments calculated from the counting distribution reveal characteristic features that are not evident in the mean and the variance (as the bimodality for off-resonant excitation), and will allow a more precise test of theoretical predictions.

The steady state of our system for off-resonant excitations and for excitation times longer than the Rydberg lifetime, has peculiar characteristics, theoretically analyzed for ultracold atoms

confined in a crystalline structure with a reduced dimensionality [30, 31, 32, 33]. A system of regularly spaced atoms excited to Rydberg states has a formal analogy with a dissipative Ising model with a transverse field and is predicted to have a dynamical phase transition between a paramagnetic and a ferromagnetic phase [29, 30, 31], with a bimodal distribution at the interfaces between dynamical phases. Our experimental results show a bimodal character for the counting distribution well before entering in the dissipative regime and in the absence of an externally imposed crystalline structure (as for instance, by an optical lattice potential). However, since the off-resonance excitation of couples of Rydberg atoms is spatially selective, over time the Rydberg excitations are expected to arrange themselves in regular arrays. Our investigation demonstrates the possibility of using ultra-cold Rydberg atoms as quantum simulators of strongly interacting many-body systems presenting locally ordered structures.

Acknowledgments

This work was supported by the E.U. through Grant No. 265031-ITN-COHERENCE and by the MIUR PRIN-2009 QUANTUM GASES BEYOND EQUILIBRIUM.

References

- [1] Gallagher T F 1994 *Rydberg Atoms* (Cambridge: Cambridge University Press)
- [2] Gallagher T F and Pillet P 2008 *Adv. At. Mol. Opt. Phys.* **56** 161
- [3] Comparat D and Pillet P 2010 *J. Opt. Soc. Am. B* **27** A208
- [4] Saffman M, Walker T G, Mølmer K 2010 *Rev. Mod. Phys.* **82** 2313
- [5] Jaksch D, Cirac J I, Zoller P, Rolston S L, Côté R and Lukin M D 2000 *Phys. Rev. Lett.* **85** 2208
- [6] Lukin M D, Fleischhauer M, Côté R, Duan L M, Jaksch D, Cirac J I and Zoller P 2001 *Phys. Rev. Lett.* **87** 037901
- [7] Urban E, Johnson T A, Henage T, Isenhowe L, Yavuz D D, Walker T G and Saffman M 2009 *Nature Phys.* **5** 110
- [8] Isenhowe L, Urban E, Zhang X L, Gill A T, Henage T, Johnson T A, Walker T G and Saffman M 2010 *Phys. Rev. Lett.* **104** 010503
- [9] Gaëtan A, Miroshnychenko Y, Wilk T, Chotia A, Viteau M, Comparat D, Pillet P, Browaeys A and Grangier P 2009 *Nature Phys.* **5** 115
- [10] Wilk T, Gaëtan A, Evellin C, Wolters J, Miroshnychenko Y, Grangier P and Browaeys A 2010 *Phys. Rev. Lett.* **104** 010502
- [11] Pohl T, Demler E and Lukin MD 2010 *Phys. Rev. Lett.* **104** 043002
- [12] Schachenmayer J, Lesanovsky I, Micheli A and Daley A J 2010 *NJP* **12** 103044
- [13] Shauß P, Cheneau M, Endres M, Fukuhara T, Hild T, Omran A, Pohl T, Gross C, Kuhr S and Bloch I 2012 *Nature* **491** 87
- [14] Cubel Liebisch T, Reinhard A, Berman P R and Raithel G 2005 *Phys. Rev. Lett.* **95** 253002 and Erratum 2007 *ibid.* **98** 109903
- [15] Reinhard A, Younge K C and Raithel G 2008 *Phys. Rev. A* **78** 060702(R)
- [16] Viteau M, Huillery P, Bason M G, Malossi N, Ciampini D, Morsch O, Arimondo E, Comparat and Pillet P 2012 *Phys. Rev. Lett.* **109** 053002
- [17] Hofmann C S, Günter G, Schempp H, Robert-de-Saint-Vincent M, Gärttner M, Evers J, Whitlock S and Weidemüller M 2013 *Phys. Rev. Lett.* **110** 203601
- [18] Mandel L 1982 *Phys. Rev. Lett.* **49** 136
- [19] Ates C, Pohl T, Pattard T and Rost J M 2007 *Phys. Rev. Lett.* **98** 023002
- [20] Amthor T, Giese C, Hofmann C S and Weidemüller M 2010 *Phys. Rev. Lett.* **104** 013001
- [21] Majumdar A, Bajcsy M, Rundquist A and Vučković J 2012 *Phys. Rev. Lett.* **108** 183601
- [22] Gustavsson S, Leturcq R, Studera M, Shorubalko I, Ihna T, Ensslin K, Driscoll D C and Gossard A C 2009 *Surf. Sci. Rep.* **64** 191
- [23] Schempp H, Günter G, Robert-de-Saint-Vincent M, Hofmann C S, Breyel D, Komnik A, Schönleber D W, Gärttner M, Evers J, Whitlock S and Weidemüller M 2014 *Phys. Rev. Lett.* **112** 013002
- [24] Malossi N, Valado M M, Scotto S, Huillery P, Pillet P, Ciampini D, Arimondo E and Morsch O 2013 *Preprint arXiv:1308.1854*
- [25] Viteau M, Radogostowicz J, Chotia A, Malossi N, Fuso F, Ciampini D, Morsch O, Ryabtsev I and Arimondo E 2010 *J. Phys. B* **43** 155301

- [26] Viteau M, Bason M, Radogostowicz J, Malossi N, Morsch O, Ciampini D and Arimondo E 2013 *Laser Phys.* **23** 015502
- [27] Dudin Y O, Li L, Bariani F and Kuzmich A 2012 *Nature Phys.* **8** 790
- [28] Binder K 1981 *Z. Phys. B* **43** 119
- [29] Weimer H, Löw R, Pfau T and Büchler H P 2008 *Phys. Rev. Lett.* **101** 250601
- [30] Ates C, Olmos B, Garrahan J P, and Lesanovsky I 2012 *Phys. Rev. A* **85** 043620
- [31] Lee T E, Häffner H, and Cross M C 2012 *Phys. Rev. Lett.* **108** 023602
- [32] Hu A, Lee T E, and Clark C 2013 *Phys. Rev. A* **88** 053627
- [33] Carr C, Ritter R, Weatherill K J, and Adams C S 2013 *Phys. Rev. Lett.* **111** 113901